

# Amplification of Cooper pair splitting current in a graphene based Cooper pair beam splitter geometry

SK Firoz Islam\* and Arijit Saha†

*Institute of Physics, Sachivalaya Marg, Bhubaneswar-751005, India and*

*Homi Bhabha National Institute, Training School Complex, Anushakti Nagar, Mumbai 400085, India*

Motivated by the recent experiments [Scientific reports, **6**, 23051 (2016), Phys. Rev. Lett. 114, 096602 (2015)], we theoretically investigate Cooper pair splitting current in a graphene based Cooper pair beam splitter geometry. By considering the graphene based superconductor as an entangler device, instead of normal (2D) BCS superconductor, we show that the Cooper pair splitting current mediated by Crossed Andreev process is amplified compared to its normal superconductor counterpart. This amplification is attributed to the strong suppression of local normal Andreev reflection process (arising from the Cooper pair splitting) from the graphene based superconductor to lead via the same quantum dot, in comparison to the usual 2D superconductor. Due to the vanishing density of states at the Dirac point of undoped graphene, a doped graphene based superconductor is considered here and it is observed that Cooper pair splitting current is very insensitive to the doping level in comparison to the usual 2D superconductor. The transport process of non-local spin entangled electrons also depends on the type of pairing *i.e.*, whether the electron-hole pairing is on-site, inter-sublattice or the combination of both. The inter-sublattice pairing of graphene causes the maximum non-local Cooper pair splitting current, whereas presence of both pairing reduces the Cooper pair splitting current.

## I. INTRODUCTION

In recent times, search for spatially separated quantum entangled states (Einstein-Podolski-Rosen pair<sup>1</sup>) in various condensed matter systems has become an exciting area of research. The generation and detection of entanglement is the prerequisite for application in the field of quantum computation and information<sup>2</sup>, quantum cryptography<sup>3</sup>, quantum teleportations<sup>4,5</sup>, and for testing Bell's inequality<sup>6</sup> etc. The two electron bound states inside a superconductor, known as Cooper pair<sup>7,8</sup>, is a natural source of entangled electron pairs. The non-local spin entangled electrons can be generated out of the superconductor by splitting this Cooper pair by means of Andreev process<sup>9</sup>. The latter is an electron-hole conversion phenomena at normal-superconductor interface. After the theoretical proposal of generating spin-entangled electrons by P. Recher et.al.<sup>10</sup>, several experiments<sup>11-14</sup> have been carried out to realize such splitting phenomena. These kind of devices are generally known as Cooper pair beam splitter (CPS) which consists of two leads attached to the superconductor at two different points via two different quantum dots in the Coulomb blockade regime. There have been several proposals of detecting spin entanglement including testing the violation of Bell's inequality<sup>6,15,16</sup>, shot noise properties<sup>17-19</sup> and Josephson current flowing through double quantum dots attached to two superconducting leads<sup>20</sup> etc.

On the other hand, graphene<sup>21</sup> is an atomically thin material of carbon atoms and its low energy spectrum is described by the massless Dirac equation rather than Schrödinger equation. Beenakker, in his seminal paper<sup>22,23</sup> has established that an undoped graphene can exhibit specular Andreev reflection (AR) in a normal-superconductor (NS) hybrid junction, which is in contrast to the usual Schrödinger type electronic systems exhibiting retro type AR. The specular AR in graphene is a direct manifestation of the two band semiconducting nature<sup>21</sup> (interband Andreev reflection) with zero band gap. Although, specular AR can also be realized in any

low (enough) gap semiconductor at low doping<sup>24</sup>. Later, J. Cayssol<sup>25</sup> has investigated quantum transport properties in a normal-superconductor-normal (NSN) hybrid junction made of graphene monolayer, and predicts that graphene could be a better candidate to realize spin-entangled electrons via the Crossed Andreev reflection (CAR) process. Very recently, graphene based CPS has been designed experimentally in order to enhance CPS current<sup>26,27</sup> compared to normal superconductor. In the experiment, superconducting correlation has been induced in graphene via the proximity effect. They have observed remarkably better performance of Cooper pair splitting by tuning gate voltage. However, these findings have been naively explained by using the theoretical work of P. Recher et al.,<sup>10</sup> which is based on BCS type 3D normal superconductor with quadratic spectrum. Hence, a microscopic theoretical analysis of graphene superconductor based CPS geometry is on demand for a better understanding of the enhancement of CPS current in it.

In this article, we intend to provide a theoretical analysis of CPS mechanism for a graphene based superconductor where pairing symmetry is considered to be originated from phonon mediated interaction and tailed by the discussions regarding proximity induced pairing. We explore the origin behind the enhancement of beam splitting process in graphene, and discuss the outcome of different kinds of pairing symmetries which are on-site, inter-sublattice and presence of both. This work is an extension of Ref. [10] to Dirac superconductor incorporating the same formalism introduced by them.

We show that the Cooper pair splitting visibility ( $\eta$ )<sup>26</sup> is amplified in Dirac like superconductor (graphene with linear spectrum) in comparison to the usual 2D BCS type superconductor with parabolic dispersion. The visibility can be defined as  $\eta = I_{CPS} / (I_{CPS} + I_{BG})$ <sup>26</sup> with  $I_{CPS}$  being the current via the two different dots and  $I_{BG}$  is the current via the same dot. The types of pairing inside the graphene superconductor play a crucial role in CPS process. The CPS visibility is minimum when only on-site pairing is present. On the other hand, it becomes maximum when only inter-sublattice pairing

is present. The presence of both types of pairing give rise to an intermediate  $\eta$ .

The remainder of the paper is organised as follows. The BCS theory for graphene is briefly reviewed in Sec. II. In Sec. III, we analytically evaluate the Cooper pair splitting current via two different dots as well as via the same dot for the graphene CPS geometry. In Sec. IV, we discuss the outcome of our analytical results. Finally, we summarize and conclude in Sec. V.

## II. BRIEF REVIEW OF BCS THEORY OF GRAPHENE

In this section, we briefly review the BCS theory of graphene superconductor as prescribed by B. Uchoa et al., in Ref. [28]. We start with the tight binding Hamiltonian for graphene as

$$H_0 = -\mu \sum_i \hat{n}_{g,i} - t \sum_{\langle ij \rangle} \sum_{s=\uparrow\downarrow} (\alpha_{is}^\dagger \beta_{js} + H.c). \quad (1)$$

Here,  $s = \uparrow, \downarrow$  denotes the spin index,  $t$  is the nearest neighbor hopping parameter ( $t \approx 2.6$  eV) between A and B sublattice,  $\alpha_i (\alpha_i^\dagger)$  is the on-site annihilation (creation) operator of electron in the A sublattice. Similarly for the B sublattice,  $\beta_i (\beta_i^\dagger)$  is the annihilation (creation) operator.  $\mu$  is the chemical potential with  $\hat{n}_{g,i}$  being the on-site particle density operator. After diagonalizing Eq.(1), the energy dispersion becomes as  $\xi_k = -t|\gamma_k|$ , where  $k$  is the 2D momentum and  $\gamma_k = \sum_{\vec{\delta}} e^{i\vec{k}\cdot\vec{\delta}}$ . Here,  $\vec{\delta} = \{\vec{\delta}_1, \vec{\delta}_2, \vec{\delta}_3\}$  are the three nearest neighbor lattice vectors. The low energy approximation at the corner of hexagonal Brillouin zone leads to the linear Dirac spectrum given by  $\xi_k = \hbar v_F |k|$  with  $v_F = (3/2)at$ -the Fermi velocity. Now we include electron-hole pairing in graphene via phonon mediated electron-electron interaction, which can be described by

$$H_{\text{int}} = \frac{g_0}{2} \sum_{is} [\alpha_{is}^\dagger \alpha_{is} \alpha_{i-s}^\dagger \alpha_{i-s} + \beta_{is}^\dagger \beta_{is} \beta_{i-s}^\dagger \beta_{i-s}] + g_1 \sum_{\langle ij \rangle} \sum_{s,s'} \alpha_{is}^\dagger \alpha_{is} \beta_{js'}^\dagger \beta_{js'}, \quad (2)$$

where  $g_0$  and  $g_1$  are the on-site and nearest neighbor electron-electron interaction strength, respectively. Introducing two types of superconducting order parameters as (a)  $s$ -wave:  $\Delta = \langle \alpha_{i\downarrow} \alpha_{i\uparrow} \rangle = \langle \beta_{i\downarrow} \beta_{i\uparrow} \rangle$  (b)  $p$ -wave:  $\Delta_{1,ij} = \langle \alpha_{i\downarrow} \beta_{i\uparrow} - \alpha_{i\uparrow} \beta_{i\downarrow} \rangle$ , the interaction terms under mean field approximation reduces to<sup>28</sup>

$$H_{\text{int}} = E_0 + g_0 \Delta \sum_i [(\alpha_{i\uparrow}^\dagger \alpha_{i\downarrow}^\dagger + \beta_{i\uparrow}^\dagger \beta_{i\downarrow}^\dagger) + H.c] + g_1 \sum_{\langle ij \rangle} \Delta_{1,ij} [(\alpha_{i\uparrow}^\dagger \beta_{j\downarrow}^\dagger - \alpha_{i\downarrow}^\dagger \beta_{j\uparrow}^\dagger) + H.c]. \quad (3)$$

Here,  $E_0 = -g_0 \Delta^2 - 3g_1 \Delta_1^2$ . In the momentum space,  $\Delta_k = \sum_{ij} \Delta_{1,ij} e^{i\vec{k}\cdot(\vec{r}_i - \vec{r}_j)} = \Delta_1 \gamma_k^*$ . In close vicinity of Dirac points, nearest neighbour order parameter can be simplified to  $\Delta = (3a/2)\Delta_1(k_y + ik_x)$  i.e., with  $\mathbf{p}+i\mathbf{p}$  symmetry. In order to decouple the two sublattices, we employ the following

transformations as<sup>29</sup>

$$\alpha_{ks} = \frac{1}{\sqrt{2}} [c_{ks} + d_{ks}] \\ \beta_{ks} = \frac{1}{\sqrt{2}} [e^{-i\phi_k} (c_{ks} - d_{ks})] \quad (4)$$

where  $c_{ks}^\dagger (d_{ks}^\dagger)$  creates an electron in the lower (upper)  $\pi$ -band. Here,  $\phi_k = \arg(\gamma_k)$ . Then after the Bogoliubov transformation, BCS Hamiltonian reduces to

$$H_{BCS} = \sum_k E_{(k,\nu=+)} \gamma_{1ks}^\dagger \gamma_{1ks} + E_{(k,\nu=-)} \gamma_{2ks}^\dagger \gamma_{2ks} \quad (5)$$

with Bogoliubov quasiparticle's energy  $E_{k,\lambda,\nu} = \lambda E_{k,\nu}$ , where  $\lambda = \pm$  and

$$E_{k,\nu} = \sqrt{(\xi_k + \nu\mu)^2 + (g_0\Delta + \nu g_1\Delta_1|\gamma_k|)^2}. \quad (6)$$

Here,  $s \equiv \uparrow\downarrow$  and  $\gamma_{1ks} (\gamma_{2ks})$  is the quasiparticle operator, corresponding to the energy  $E_{k,+}$  ( $E_{k,-}$ ) which can be linked to the annihilation and creation operators as

$$c_{k,\nu,\uparrow} = u_{k,\nu} \gamma_{1k\uparrow} + v_{\nu,k} \gamma_{1-k\downarrow}^\dagger \quad (7)$$

$$c_{-k,\nu,\downarrow} = u_{k,\nu} \gamma_{1-k\downarrow} - v_{\nu,k} \gamma_{1k\uparrow}^\dagger \quad (8)$$

with the quasiparticle weights  $u_{k,\nu} = (1/\sqrt{2})(1 + \xi_k/E_{k,\nu})^{1/2}$ , and  $v_{k,\nu} = (1/\sqrt{2})(1 - \xi_k/E_{k,\nu})^{1/2}$ . Note that, unlike normal superconductor, graphene superconductor exhibits two kinds of Bogoliubov quasiparticles in each band with different energies denoted by  $\nu$ . The appearance of two types of Bogoliubov quasiparticles with different energies is in complete contrast to usual normal BCS superconductor where Bogoliubov quasiparticle is of one type. This unusual feature of Bogoliubov quasiparticle in graphene is going to play an important role in graphene based CPS geometry. Here we investigate three different cases:

(a) Intra-sublattice pairing i.e.,  $\Delta \neq 0$  and  $\Delta_1 = 0$ : In this case, the superconductor is described by the gap  $2|g_0\Delta|$ . Note that, this on-site pairing is also equivalent to proximity induced pairing in graphene<sup>22</sup>.

(b) Inter-sublattice pairing i.e.,  $\Delta = 0$  and  $\Delta_1 \neq 0$ : In this case, the hopping parameter and the chemical potential are renormalized as

$$t' = \sqrt{t^2 + g_1^2 \Delta_1^2} \quad (9)$$

and

$$\mu' = \frac{\mu t}{\sqrt{t^2 + g_1^2 \Delta_1^2}}. \quad (10)$$

Hence, the quasiparticle's energy reduces to

$$E_{k,\nu} = \sqrt{(t'|\gamma_k| + \nu\mu')^2 + \Delta'^2} \quad (11)$$

with gap  $\Delta' = \mu g_1 \Delta_1 / \sqrt{t^2 + g_1^2 \Delta_1^2}$ . Note that, superconducting gap vanishes for undoped graphene ( $\mu = 0$ ). So this kind

of pairing is intrinsically related to finite doping.

(c) Presence of both the pairings *i.e.*,  $\Delta \neq 0$  and  $\Delta_1 \neq 0$ : In this case, the energy gap turns out to be  $2|tg_0\Delta - g_1\mu\Delta_1|/\sqrt{t^2 + g_1^2\Delta_1^2}$  with renormalized chemical potential

$$\mu' = (t\mu + g_0g_1\Delta\Delta_1)/\sqrt{t^2 + g_1^2\Delta_1^2}. \quad (12)$$

Because of the vanishing density of states at the Dirac point, realization of superconductivity in undoped graphene is difficult. Hence one has to tune the chemical potential substantially above the Dirac points which can be done by chemically doping the graphene with metal coating as mentioned in Ref. [28].

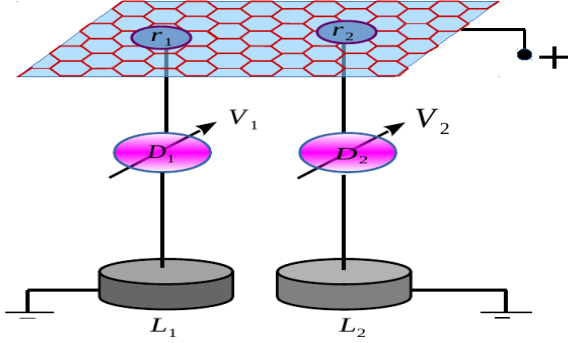


Figure 1. (Color online) Schematic of the Cooper pair beam splitter device based on the graphene superconductor. Two quantum dots are denoted by  $D_1$  and  $D_2$ . Leads are shown by two circular disks and referred by  $L_1$  and  $L_2$ . Two gate voltages  $V_1$  and  $V_2$  are coupled to the two dots to tune the energy levels of the dots.

### III. GRAPHENE BASED COOPER PAIR BEAM SPLITTER

In this section, we analytically evaluate the Cooper pair splitting current following the route given in Ref. [10] for the normal 3D BCS superconductor. Before proceeding further we characterize our device with different scattering processes and required conditions. The mechanisms which are involved in the beam splitting phenomena are the Andreev processes and Coulomb blockade effects. We consider that the graphene superconductor is kept at a chemical potential  $\mu_S$ , and weakly coupled to two separate leads via two quantum dots as shown schematically in Fig. 1. Note that, to avoid edge effect of graphene, we consider contact points much inside the graphene sheet. Two quantum dots are denoted by  $D_1$  and  $D_2$ , while the two normal leads are denoted by  $L_1$  and  $L_2$ , respectively. Two leads are kept at the same chemical potential *i.e.*,  $\mu_1 = \mu_2 = \mu$ , where  $\mu_1$  and  $\mu_2$  refer to the chemical potential of lead 1 and lead 2, respectively. Transport of entangled electrons occurs under the bias voltage  $\Delta\mu = \mu_S - \mu_l > 0$ , where  $l = 1, 2$  denote lead  $L_1$  and  $L_2$ , respectively. The single particle energy levels  $\epsilon_1$  and  $\epsilon_2$  of the two quantum dots can be tuned externally via gate voltage ( $D_1$  and  $D_2$ ) to satisfy resonance condition, described by two particle Breit-Wigner peak

at  $\epsilon_1 + \epsilon_2 = 2\mu_S$ . The latter describes the co-tunneling of two electrons into two different dots. To block the unwanted correlation between electrons, already present on the quantum dots and electron coming from superconductor, one would work in the co-tunneling regime in which the number of electrons on the dots are fixed and the resonant levels  $\epsilon_l$  cannot be occupied. To prevent the spin flip process energy level spacing of quantum dots has to be higher than thermal energy  $k_B T$  and bias voltage  $\Delta\mu$ , where  $k_B$  and  $T$  are the Boltzmann constant and temperature, respectively. The electron that enters into the dots from the superconductor must leave the dot to lead much faster than the time scale in which another electron arrives into the dots *i.e.*,  $|T_{SD}| < |T_{DL}|$ , where  $T_{SD}$  is the tunneling amplitude from superconductor to dot and  $T_{DL}$  is the tunneling amplitude from dot to superconductor, respectively. The superconducting energy gap also characterizes the time delay between two successive Andreev tunneling events of the two electrons of a Cooper pair. In order to suppress the single electron tunneling where the creation of the quasiparticle in the superconductor is a final excited state, one require that  $\Delta > \Delta\mu, k_B T$ . The Hamiltonian of the entire system is described by

$$H = H_{BCS} + \sum_I H_{DI} + \sum_I H_{LI} + H_T \quad (13)$$

with  $I = 1, 2$ . Here, the superconductor is described by the graphene BCS Hamiltonian with  $\gamma_v|0\rangle_v = 0$ . Both dots are modeled as Anderson-type Hamiltonian given by  $H_{DI} = \epsilon_l \sum_s d_{ls}^\dagger d_{ls} + U n_{\uparrow} n_{\downarrow}$ , where  $U$  is the Coulomb blockade energy. Only resonant levels of the dots participate in transport phenomenon here.

The leads are assumed to be non-interacting Fermi liquids with the Hamiltonian  $H_{LI} = \sum_{ks} \epsilon_k a_{lks}^\dagger a_{lks}$ . Tunneling from superconductor to dots and dots to leads are described by the tunneling Hamiltonian  $H_T = H_{SD} + H_{DL}$  given as

$$H_{SD} = \sum_{ls} T_{SD} d_{ls}^\dagger \psi_s(\vec{r}_l) + h.c \quad (14)$$

and

$$H_{DL} = \sum_{lks} T_{DL} a_{lks}^\dagger d_{lks} + h.c \quad (15)$$

The field operators are given by  $\psi_s(\vec{r}_l) = \sum_k e^{i\vec{k}\cdot\vec{r}_l} c_{ks}$  or  $\sum_k e^{i\vec{k}\cdot\vec{r}_l} d_{ks}$  depending on type of Bogoliubov quasi particles.

The Cooper pair splitting current from superconductor to the dots is given by

$$I = 2e \sum_{f,i} W_{fi} \rho_i \quad (16)$$

with the transition rate

$$W_{fi} = 2\pi |\langle f|T(\epsilon_i)|i\rangle|^2 \delta(\epsilon_f - \epsilon_i). \quad (17)$$

Here,  $T(\epsilon_i) = H_T G(E)(\epsilon_i - H_0)$  is the on shell transmission or T-matrix with  $G(E) = [\epsilon_f + i0 - H]^{-1}$ . The initial occupation probability for the entire system in states  $|i\rangle$  is denoted

by  $\rho_i$ . The T-matrix can be written as a power series in tunnel Hamiltonian as<sup>10</sup>

$$T(\epsilon_i) = H_T + H_T \sum_{n=1} [G(E)H_T]^n. \quad (18)$$

The initial state is defined as  $|i\rangle = |0\rangle_S |0\rangle_D |\mu_i\rangle$ , where  $|0\rangle$  is the quasiparticle vacuum for the superconductor. Furthermore,  $\gamma_S = 2\pi v_S |T_{SD}|^2$  and  $\gamma_I = 2\pi v_I |T_{DL}|^2$  ( $I = 1, 2$ ) denote the tunneling rates between superconductor and dots and between dots and leads, respectively. Also,  $v_S$  and  $v_I$  are the density of states of graphene and the leads, respectively.

### A. Current via two dots

Here, we analytically evaluate the current due to simultaneous transport of two electrons via two different dots. This process is known as the crossed Andreev reflection in literature. The two electrons coming out of the graphene superconductor can be either singlet ( $S=0$ ) or triplet ( $S=1$ ). The conservation of the total spin  $S$ ,  $[\mathbf{S}^2, H] = 0$ , guarantees the preservation of the singlet or triplet states of Cooper pair during the transport process via two dots into the leads. The final states of the two electrons, in two different leads, are described by the quantum state  $|f\rangle = (1/\sqrt{2})[a_{1p\uparrow}^\dagger a_{2q\downarrow}^\dagger \pm a_{1p\downarrow}^\dagger a_{2q\uparrow}^\dagger]|i\rangle$ , where  $-$  and  $+$  denote singlet and triplet, respectively. Here,  $p$  and  $q$  are the momentum vector in two leads corresponding to the energy  $\epsilon_p$  and  $\epsilon_q$ , respectively. Also,  $a_{1ps}^\dagger$  is the creation operator of electron with spin  $s$  in lead 1 with momentum  $p$ , whereas  $a_{2qs}^\dagger$  denotes the same for lead 2 with momentum  $q$ . After splitting of the Cooper pair, one electron with spin  $\uparrow$  ( $\downarrow$ ) migrates to dot 1 from the contact point  $r_1$  of superconductor. The second electron with spin  $\downarrow$  ( $\uparrow$ ) from contact point  $r_2$  migrates to the dot 2 before the electron with spin  $\uparrow$  ( $\downarrow$ ) in the dot 1 escapes to lead 1. The matrix element for the final states being singlet in dots, can be directly obtained following Ref. [10] as

$$M_{SD} = \frac{4T_{SD}^2}{\epsilon_1 + \epsilon_2 - i\eta} \sum_{k,\nu} \frac{u_{k,\nu} v_{k,\nu}}{E_{k,\nu}} \cos(\mathbf{k} \cdot \delta \mathbf{r}), \quad (19)$$

where  $\delta \mathbf{r} = \mathbf{r}_1 - \mathbf{r}_2$  denotes the separation between the two contact points inside the superconductor from which electrons 1 and 2 tunnel into the dots. To evaluate the sum over  $k$  [see Appendix A for details], we use  $u_{k,\nu} v_{k,\nu} = \Delta / (2E_{k,\nu})$ . Note that, the expression in Eq.(19) is similar as Ref. [10] except an additional summation over index  $\nu$  attributed to two different branches of Bogoliubov quasi particles for graphene superconductor. After linearizing the energy dispersion around the Fermi level, the summation can be reduced to

$$\sum_{k,\nu} \frac{u_{k,\nu} v_{k,\nu}}{E_{k,\nu}} \cos(\mathbf{k} \cdot \delta \mathbf{r}) = \frac{\pi}{2} v_s^g \kappa^g(k_F \delta r). \quad (20)$$

Here,  $k_F$  is the Fermi momentum at chemical potential  $\mu_s$ , and the density of states of graphene  $v_s^g = \mu_s / [2\pi(\hbar v_F)^2]$ . Here, in above equation

$$\kappa^g(x) = \frac{1}{\pi} [gK_0(gx) + g^* K_0(g^*x)], \quad (21)$$

where  $K_0$  is the zeroth order modified Bessel function,  $g = [1/(\pi \xi_1^g k_F) + i]$  and  $\xi_1^g = \hbar v_F / (\pi \Delta)$  is the superconducting coherence length. Now, if we evaluate the same for usual 2D superconductor (only single energy branch), then

$$\sum_k \frac{u_k v_k}{E_k} \cos(\mathbf{k} \cdot \delta \mathbf{r}) = \frac{\pi}{2} v_s^{2d} \kappa^{2d}(k_F \delta r). \quad (22)$$

Here,

$$\kappa^{2d}(x) = \frac{1}{\pi} [K_0(\omega^* x) - K_0(\omega x)] \quad (23)$$

with  $\omega = [1 + \{2/(\pi k_F \xi_1^{2d})\}^2]^{1/2} \exp(i\theta/2)$  and  $\cot \theta = \pi k_F \xi_1^{2d} / 2$ . Also,  $v_s^{2d} = m^* / 2\pi \hbar^2$  is the density of states of usual 2D electronic systems with  $m^*$  is the effective mass of electron and  $\xi_1^{2d}$  is the coherence length of usual 2D superconductor. Note that the coherence length of graphene superconductor is higher than usual 2D superconductor because of the higher Fermi velocity. It can also be seen that tunneling amplitude is less sensitive to the coherence length in usual 2D superconductor than graphene superconductor. An approximate form of the transmission amplitude for usual 2D superconductor is given in Ref. [30]. However, to draw a comparison with graphene we need exact result.

Furthermore, we look into the case of the transmission amplitude from dots to leads. The current from dots to Fermi liquid leads is given by<sup>10</sup>

$$M_{DL} = -T_{DL}^2 \frac{\epsilon_1 + \epsilon_2 - i\eta}{(\epsilon_1 + \epsilon_q - i\gamma_1)(\epsilon_2 + \epsilon_p - i\gamma_2/2)}. \quad (24)$$

However, for our particular case of graphene based superconductor, a factor of 2 should be multiplied to capture the contribution from two different kinds of Bogoliubov quasiparticles. After performing integration over momentum  $p$  and  $q$  of leads, the current via the two dots becomes

$$I_{CPS} = \frac{e\gamma_s^2 \gamma}{(3\mu_s)^2 + (\gamma/2)^2} |k^g(k_F \delta r)|^2 \quad (25)$$

with  $\gamma = \gamma_1 + \gamma_2$  is the total tunneling rate between dots to leads. Note that, unlike usual 2D superconductor where density of states is constant and does not depend on energy, it is directly proportional to the Fermi level in graphene for which a substantial doping or suitable gating is necessary to make Cooper pair available for transport process, otherwise at the Dirac point  $I_{CPS} \simeq 0$  due to the unavailability of density of states. For the case of inter-site pairing, we obtain the similar results with the appropriate rescaling of hopping parameter and chemical potential.

### B. Current via same dot

In this subsection, we analytically compute current via the same dots, which can occur via two possible scattering processes, (i) one electron with spin-up tunnels to dot 1 from

graphene superconductor and then second electron with spin-down also tunnels to dot 1. When the two electrons with opposite spins are in the same dot, then that process costs an additional energy  $U$ . This process is the usual local Andreev reflection. (ii) One electron tunnels to dot 1 and then go to lead 1 before another electron from the graphene superconductor arrives at dot 1. First we consider the second process. Following Ref. [10], we begin with the transmission matrix

$$\begin{aligned} \langle f|T_0|i\rangle &= \sum_{p''s} \langle f|H_{DL}|D''s\rangle \langle Dp''s| \sum_{n=0} \left( \frac{1}{i\eta - H_0} H_{DL} \right)^{2n} |Dp''s\rangle \\ &\langle Dp''s| \frac{1}{i\eta - H_0} H_{SD} \frac{1}{i\eta - H_0} H_{DL} \frac{1}{i\eta - H_0} H_{SD} |i\rangle \end{aligned} \quad (26)$$

First two matrix elements in the above equation correspond to the transition between dot to lead, which will be remained same as the leads are kept unchanged, and was already evaluated in Ref. [10]. The last matrix element involves the graphene superconductor Hamiltonian ( $H_{SD}$ ), for which we evaluate it as [see Appendix B for details]

$$\begin{aligned} \langle Dp''s| \frac{1}{i\eta - H_0} H_{SD} \frac{1}{i\eta - H_0} H_{DL} \frac{1}{i\eta - H_0} \\ H_{SD} |i\rangle &= \pm \frac{T_{DL} T_{SD}^2 v_s^g}{(\epsilon_l + \epsilon_{p''} - i\eta) \mu_s} \frac{2}{\mu_s}. \end{aligned} \quad (27)$$

Here, +(-) sign corresponds to spin-up (down). Substitution of this expression into the transmission amplitude yields

$$\langle f|T_0|i\rangle = - \frac{2\sqrt{2}v_s^g (T_{SD} T_{DL})^2 (\epsilon_l - i\gamma_l/2)}{(\epsilon_l + \epsilon_p - i\gamma_l/2)(\epsilon_l + \epsilon_{p''} - i\gamma_l/2) \mu_s} \frac{2}{\mu_s}. \quad (28)$$

In usual 2D/3D normal BCS superconductor, it gives similar results except  $v_s^g/\mu_s$  is replaced by  $v_s^d/\Delta$ . Hence, this process is suppressed by the factor  $[2\pi(\hbar v_F)^2]^{-1}$  in graphene based superconductor in comparison to usual 2D superconductor where it is suppressed by  $m^*(2\pi\hbar^2\Delta)^{-1}$ . Due to the higher Fermi velocity in graphene, the degree of suppression of this process is higher in graphene based superconductor than usual 2D BCS superconductor.

Now, we consider the first case, where two electrons tunnel together from the superconductor to dot and because of the Coulomb blockade phenomena it costs additional energy  $U$ . In this process, the matrix element involving superconducting Hamiltonian can be evaluated by just replacing  $\Delta$  by  $U/\pi$  in normal superconductor. However, in graphene we evaluate it to be as

$$\begin{aligned} \langle Dp''s| \frac{1}{i\eta - H_0} H_{DL} \frac{1}{i\eta - H_0} H_{SD} \frac{1}{i\eta - H_0} \\ H_{DL} |i\rangle &= v_s^g \frac{\Delta}{2U\mu_s} \sum_v \ln \left[ 1 + \left( \frac{\epsilon_c - \nu\mu_s}{\Delta} \right)^2 \right] \end{aligned} \quad (29)$$

Here,  $\epsilon_c$  is the energy cut-off inside the superconductor. Due to the cumulative effect of these two processes, the current via the same dot is found to be

$$I_{BG} = 2e \frac{\gamma_s^2 \gamma}{A} B, \quad (30)$$

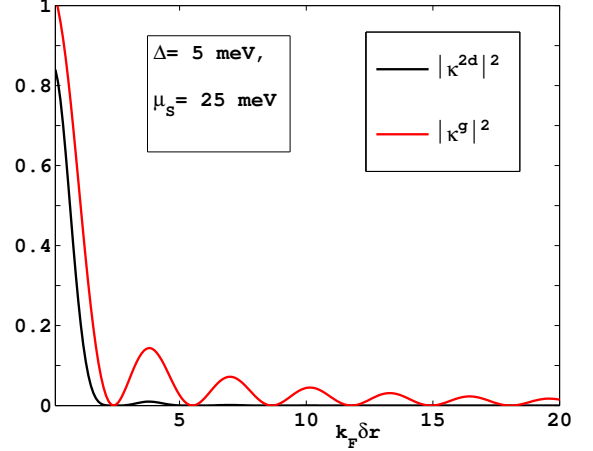


Figure 2. (Color online) The behavior of square of the transmission amplitudes for graphene and usual 2D BCS superconductor are shown as a function of  $k_F \delta r$ . Here,  $\delta r$  is the separation between the two electrons of the Cooper pair inside the graphene sheet.

where

$$B = \frac{2}{\pi\mu_s} + \frac{\Delta}{2U\pi\mu_s} \sum_v \ln \left[ 1 + \left( \frac{\epsilon_c - \nu\mu_s}{\Delta} \right)^2 \right]. \quad (31)$$

So the efficiency of Cooper pair splitting for graphene based superconductor (using resonance condition  $\epsilon_1 + \epsilon_2 = 2\mu_s$ ) becomes

$$\frac{I_{CPS}}{I_{BG}} = \frac{A}{2B} |\kappa^g(k_F \delta r)|^2. \quad (32)$$

with

$$A = \frac{(3\mu_s)^2 + (\gamma/2)^2}{[6\mu_s^2 + (\gamma/2)^2]^2 + [5\mu_s\gamma/2]^2} \quad (33)$$

and for usual 2D superconductor, the same turns out to be

$$\frac{I_{CPS}}{I_{BG}} = \frac{A\mathcal{E}^2}{2} |\kappa^{2d}(k_F \delta r)|^2 \quad (34)$$

with  $1/\mathcal{E} = 1/U + 1/(\pi\Delta)$ .

#### IV. RESULTS AND DISCUSSION

In this section, we discuss our results for graphene based Cooper pair beam splitter geometry in comparison to that of the usual 2D BCS superconductor. First, we show a comparative behavior of tunneling probability for the process A (two electrons tunnel via two different dots) in Fig. 2. Note that, we use  $\Delta$  and  $\Delta_1$  in units of  $g_0$  and  $g_1$ , respectively for numerical plots. Both of them exhibits oscillatory behavior. Nevertheless, in case of normal 2D superconductor, the amplitude of oscillation decays much faster than graphene superconductor. It also shows that the tunneling probability for process A in

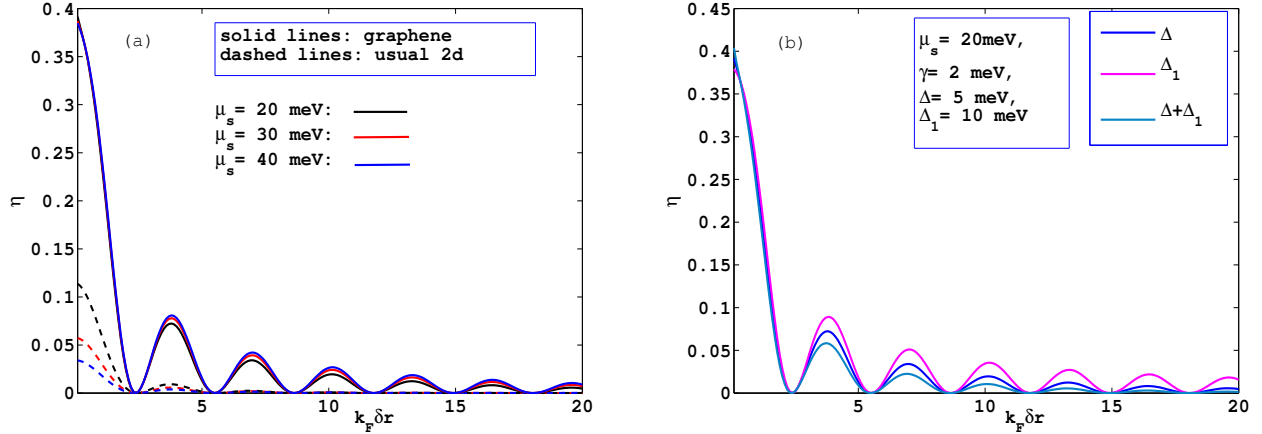


Figure 3. (Color online) CPS visibility ( $\eta$ ) is illustrated as a function of  $k_F \delta r$ . In panel (a) results are shown for graphene and usual 2D superconductor together for various values of doping. On the other hand, in panel (b) results are demonstrated for different kinds of pairing symmetry in graphene based superconductor.

graphene is higher in magnitude compared to usual 2D superconductor. The Cooper pair splitting probability via two dots survives for a relatively wide range of the distance ( $\delta r$ ) between two dots-superconductor contact points as far as the graphene is concerned. The origin of this survival can be attributed to the large coherence length and the presence of two types of Bogoliubov quasiparticles in graphene instead of one type of them in normal 2D superconductor. Since the non-local transport occurs via Crossed Andreev reflection process, as pointed out in Sec. III, to draw a clear comparison of performances between graphene based CPS and usual 2D superconductor based CPS we explore the CPS visibility, introduced in Ref. [26], as

$$\eta = \frac{I_{CPS}}{I_{CPS} + I_{BG}}. \quad (35)$$

In the second case of process B (two electrons tunnel sequentially via same dot), we find that non-local transport is suppressed by  $v_s^g/\mu_s = [2\pi(\hbar v_F)^2]^{-1}$ , whereas in normal 2D BCS superconductor it is  $v_s^{2d}/\Delta = m^*/[2\pi\hbar^2\Delta]$ . Such suppression in graphene is governed by the factor  $1/v_F^2$  and in normal 2D superconductor its counterpart is  $m^*/\Delta$ . Hence, it can be clearly understood that suppression in graphene is much stronger than usual 2D superconductor as  $v_F > \sqrt{\Delta/m^*}$ . On the other hand, the first case of process B, where two electrons tunnel via same dot simultaneously, costs additional energy  $U$  and is suppressed by  $v_s^{2d}/U$  in usual 2D superconductor. On the contrary, in case of graphene based superconductor it is  $v_s^g \frac{\Delta}{2U\mu_s} \sum_v \ln \left[ 1 + \left( \frac{\epsilon_c - v\mu_s}{\Delta} \right)^2 \right]$ . Note that, in the latter case, suppression does not differ significantly in two systems for the same density of states and  $\epsilon_c \sim 30\Delta$ .

In Fig. 3, we show CPS visibility as a function of  $k_F \delta r$ . A comparative analysis between the graphene and the usual 2D superconductor based CPS is demonstrated in Fig. 3(a). It can be observed that CPS visibility in graphene superconductor is higher in magnitude and insensitive to the change of

chemical potential than normal 2D superconductor case. The origin of higher CPS visibility can be understood from the fact that current via the same dot is more suppressed in graphene compared to the usual 2D superconductor as explained earlier. In addition to that, higher transmission probability via two different dots in graphene based superconductor is also responsible for higher CPS visibility than normal 2D BCS superconductor. In Fig. 3(b), we also illustrate the features of CPS visibility in graphene superconductor with  $k_F \delta r$  but for different kinds of pairing symmetry. We consider inter-sublattice pairing ( $\Delta_1$ ) is stronger than on-site pairing  $\Delta$  as in isotropic  $k$ -space on-site pairing is less favoured due to strong Coulomb repulsion<sup>31</sup>. It is observed that maximum CPS visibility is achieved only when inter-sublattice pairing is present. The on-site pairing gives rise to relatively less CPS visibility in comparison to inter-sublattice pairing. In another situation, when both types of pairing are present, CPS visibility exhibits a minimum value in comparison to other two individual pairings. Note that, so far our discussion is restricted to phonon-mediated pairing. The variation of CPS visibility with respect to pairing symmetry is related to the effective superconducting gap as well as effective chemical potential as discussed in the last paragraph of Sec. II. The proximity induced pairing can be captured by the on-site pairing, which has been considered in Ref. [22] in analyzing specular Andreev reflection in graphene. The inter-sublattice pairing arises exclusively due to phonon-mediated superconductivity in graphene. On the other hand, intra-sublattice pairing can be present in both mechanisms (proximity induced superconductivity as well as phonon mediated electron-electron interaction induced superconductivity).

Here we present a comparative discussion between our theoretical results and the experiments (Refs. [26 and 27]). First, in experimental set up (Refs. [26 and 27]), superconductivity has been induced in a graphene sample via the proximity effect. They have used Al (normal BCS superconductor) to in-

duce superconductivity in graphene monolayer. On the other hand, we have considered various microscopic phonon mediated pairing symmetries in graphene. Nevertheless, the proximity induced gap is analogous to our on-site (intra-sublattice) pairing gap  $\Delta$ , for which our analysis can also be mapped to proximitized graphene based CPS geometry. Secondly, in Ref. [26], there is evidence of having visibility ( $\eta$ ) ranging from 0.5 – 0.86 which is quite justified by our analysis also considering low  $k_F$  and intra-sublattice pairing gap  $\Delta$ . However, in those experiments (Refs. [26 and 27]), two quantum dots are also fabricated on the same sample *i.e.*, superconducting graphene lead and dots are in the same plane. In those experimental CPS devices, edge effects cannot be ignored. On the other hand, in order to avoid the disturbances caused by the edge effects, we have modeled our CPS device in such way that the two quantum dots are directly tunnel coupled to the bulk of the graphene superconductor, as depicted in Fig. 1.

Finally we discuss if graphene based superconductor can have any significant impact on electrical noise measurement as a test of entanglement, proposed by P. Samuelson et al., in Ref. [19]. It has already been pointed out in Ref. [19], that the form of tunneling amplitude from the superconductor to leads does not play any significant role in noise measurement. The auto-correlation between two electrons in normal Andreev process appears to be<sup>19</sup>

$$S_{AA} = S_{BB} = \frac{4e^2}{h} \int_{-eV}^{eV} dE \{ [1+2RT]|A(E)|^2 + 2RTA(E)A^*(-E) \}. \quad (36)$$

On the other hand, the cross-correlation between two entangled electrons via the CAR process can be written as

$$S_{AB} = S_{BA} = \frac{4e^2}{h} \int_{-eV}^{eV} dE \{ [T^2+R^2]|A(E)|^2 - 2RTA(E)A^*(-E) \} \quad (37)$$

with

$$A(E) = \frac{|\kappa^{g/2d}| \gamma}{(E + \epsilon_1 - i\gamma/2)(-E + \epsilon_2 - i\gamma/2)}, \quad (38)$$

where,  $R = |r|^2$  and  $T = 1 - R$ . Note that, the above expression (Eq.(37)) is valid for two electrons tunneling through two different dots. Also, here  $E = \epsilon_q = \epsilon_p$ . In the above Eqs. (36-37), the energy integration of the last term yields

$$\int dE A(E)A^*(-E) = \frac{4\pi|\kappa^{g/2d}|^2 \gamma}{4\mu_S^2 + \gamma^2}. \quad (39)$$

This integration determines the degree of bunching which corresponds to the suppression of cross-correlations and enhancement of auto-correlations. The bunching behavior of shot noise is the indication of spin singlet electrons coming out of the entangler, which can be detectable in experiment. The degree of bunching in the shot noise for graphene and usual 2D superconductor is governed by the strength of  $\kappa^g$  and  $\kappa^{2d}$ , respectively. From the Fig. 2, it can be seen that tunneling amplitude for graphene is relatively stronger in comparison to usual 2D superconductor. Hence the degree of

bunching in noise measurement in graphene based beam splitter would be much stronger in comparison to usual 2D superconductor, making the possible entangled state detection more feasible in case of graphene.

## V. SUMMARY AND CONCLUSIONS

To summarize, in this article, we investigate the CPS device based on a graphene superconductor. Our analysis is motivated by two recent experiments on graphene based Cooper pair splitter device<sup>26,27</sup>. We use the fact that unlike normal BCS type superconductor, the hexagonal lattice structure of graphene exhibits two types of Bogoliubov quasiparticles with different energy. We find that graphene based superconductor can amplify the Cooper pair beam splitting visibility, which is also the main claim of the experiments. The amount of amplification also depends on the type of pairing. The inter sublattice pairing, originated from the electron-phonon interaction in graphene, causes maximum beam splitting visibility in comparison to on-site pairing. The latter type of pairing can arise due to both proximity induced superconductivity and electron-phonon interaction. However, for experimental situation, the proximity induced superconductivity is the only realistic possibility<sup>26,27</sup>. When both types of pairing are considered, CPS visibility exhibits a minimum. We also observe that the origin behind this amplification lies in the fact of strong suppression of electron tunneling via the same dots and corresponding enhancement of CPS current via two different dots in comparison to the normal 2D BCS superconductor. We also notice that CPS visibility is very insensitive to doping level in graphene in comparison the normal 2D superconductor. Finally, we discuss that the degree of electrical noise bunching, a signature of entangled states, is expected to be stronger for graphene based CPS device rather than usual 2D superconductor.

## ACKNOWLEDGMENTS

SFI acknowledges Arijit Kundu for useful discussions.

### Appendix A: Transmission matrix for electrons tunneling from superconductor to two different dots

Here, we simplify the matrix element corresponding to the CPS current via two different dots (see Eq.(19)) as

$$M_{SD} = \frac{4T_{SD}^2}{\epsilon_1 + \epsilon_2 - i\eta} \sum_{k,v} \frac{u_{k,v} v_{k,v}}{E_{k,v}} \cos(\mathbf{k} \cdot \delta \mathbf{r}), \quad (A1)$$

The summation over  $k$  can be evaluated as follows:

$$\sum_{k,v} \frac{u_{k,v} v_{k,v}}{E_{k,v}} \cos(\mathbf{k} \cdot \delta \mathbf{r}) = \frac{\Delta}{4\pi} \sum_v \int_0^\infty \frac{k dk}{E_{k,v}^2} J_0(k\delta r). \quad (A2)$$

Here,  $J_0(k\delta r)$  is the zeroth-order Bessel function of first kind. We have also used  $u_{k,v} v_{k,v} = \Delta/2E_{k,v}$ . Note that  $\Delta$  is the superconducting gap, and for different types of pairing it has to be

rescaled accordingly as discussed in Sec. II. Here, we use the well known convolution theory for Laplace transformation

$$\int_0^{\infty} f(x)h(x)dx = \int_0^{\infty} (\mathcal{L}f)(s).(\mathcal{L}^{-1}h)(s)ds, \quad (\text{A3})$$

to evaluate the integral in Eq.(A2). After using  $\mathcal{L}J_0(k\delta r) = 1/\sqrt{s^2 + \delta r^2}$  and the identity of modified Bessel function of zeroth order

$$K_0(gx) = \int_0^{\infty} \frac{\cos(g\rho)}{\sqrt{\rho^2 + x^2}} d\rho, \quad (\text{A4})$$

it is straightforward to have

$$\sum_k \frac{u_{k,v}v_{k,v}}{E_{k,v}} \cos(\mathbf{k}.\delta\mathbf{r}) = \frac{\pi}{2} v_s^g k^g (k_F \delta r). \quad (\text{A5})$$

Similarly for usual 2D superconductor

$$\sum_k \frac{u_k v_k}{E_k} \cos(\mathbf{k}.\delta\mathbf{r}) = \frac{\Delta}{4\pi} \sum \int_0^{\infty} \frac{kd k}{E_k^2} J_0(k\delta r). \quad (\text{A6})$$

Following the same approach, we obtain

$$\sum_k \frac{u_k v_k}{E_k} \cos(\mathbf{k}.\delta\mathbf{r}) = \frac{\pi}{2} v_s^{2d} k^{2d} (k_F \delta r). \quad (\text{A7})$$

## Appendix B: Evaluation of the transmission matrix for two electrons tunneling via the same dot

To evaluate the following matrix elements

$$\langle Dp'' | \frac{1}{i\eta - H_0} H_{SD} \frac{1}{i\eta - H_0} H_{DL} \frac{1}{i\eta - H_0} H_{SD} | i \rangle \quad (\text{B1})$$

we use the following two complete sets of vector

$$\sum_{k'p's} \gamma_{k's}^\dagger a_{p'-s}^\dagger |i\rangle \langle i| a_{p'-s} \gamma_{k's} = 1 \quad (\text{B2})$$

$$\sum_{k's} \gamma_{k's}^\dagger d_{-s}^\dagger |i\rangle \langle i| d_{-s} \gamma_{k's} = 1 \quad (\text{B3})$$

between  $H_{SD}$  and  $H_{DL}$ ; and between  $H_{DL}$  and  $H_{SD}$ , respectively. Then we obtain

$$\begin{aligned} & \langle Dp'' s | \frac{1}{i\eta - H_0} H_{SD} \frac{1}{i\eta - H_0} H_{DL} \frac{1}{i\eta - H_0} H_{SD} | i \rangle \\ &= \pm \frac{T_{DL} T_{SD}^2}{(\epsilon_l + \epsilon_{p''} - i\eta)} \sum_{k,v} \frac{1}{E_{k,v}^3}, \end{aligned} \quad (\text{B4})$$

where  $\sum_{k,v} [E_{k,v}]^{-3} = 2v_s^g/\mu_s$ . In case of normal 2D superconductor,  $\sum_k [E_k]^{-3} = v_s^{2d}/\Delta$ . In the other case, when two electrons migrate together to the same dot from superconductor, then this process costs an additional Coulomb energy  $U$ . Hence, the corresponding matrix element yields

$$\begin{aligned} & \langle Dp'' s | \frac{1}{i\eta - H_0} H_{DL} \frac{1}{i\eta - H_0} H_{SD} \frac{1}{i\eta - H_0} H_{DL} | i \rangle \\ &= v_s^g \frac{\Delta}{2U\mu_s} \sum_v \left[ \ln \left\{ 1 + \left( \frac{\epsilon_c + v\mu_s}{\Delta} \right)^2 \right\} \right]. \end{aligned} \quad (\text{B5})$$

\* firoz@iopb.res.in

† arijit@iopb.res.in

<sup>1</sup> A. Einstein, B. Podolsky, and N. Rosen, Phys. Rev. **47**, 777 (1935).

<sup>2</sup> M. A. Nielsen and I. Chuang, "Quantum computation and quantum information (cambridge university press, cambridge)," (2002).

<sup>3</sup> N. Gisin, G. Ribordy, W. Tittel, and H. Zbinden, Rev. Mod. Phys. **74**, 145 (2002).

<sup>4</sup> C. H. Bennett, G. Brassard, C. Crépeau, R. Jozsa, A. Peres, and W. K. Wootters, Phys. Rev. Lett. **70**, 1895 (1993).

<sup>5</sup> D. Boschi, S. Branca, F. De Martini, L. Hardy, and S. Popescu, Phys. Rev. Lett. **80**, 1121 (1998).

<sup>6</sup> J. S. Bell, Rev. Mod. Phys. **38**, 447 (1966).

<sup>7</sup> J. Bardeen, L. N. Cooper, and J. R. Schrieffer, Phys. Rev. **106**, 162 (1957).

<sup>8</sup> M. Tinkham, *Introduction to superconductivity* (Courier Corporation, 1996).

<sup>9</sup> A. F. Andreev, Zh. Eksp. Teor. Fiz. **46**, 1823 (1964).

<sup>10</sup> P. Recher, E. V. Sukhorukov, and D. Loss, Phys. Rev. B **63**, 165314 (2001).

<sup>11</sup> L. Hofstetter, S. Csonka, J. Nygård, and C. Schönberger, Nature **461**, 960 (2009).

<sup>12</sup> L. G. Herrmann, F. Portier, P. Roche, A. L. Yeyati, T. Kontos, and C. Strunk, Phys. Rev. Lett. **104**, 026801 (2010).

<sup>13</sup> A. Das, Y. Ronen, M. Heiblum, D. Mahalu, A. V. Kretinin, and H. Shtrikman, Nature communications **3**, 1165 (2012).

<sup>14</sup> G. Fülöp, F. Domínguez, S. d'Hollosy, A. Baumgartner, P. Makk, M. H. Madsen, V. A. Guzenko, J. Nygård, C. Schönberger, A. Levy Yeyati, and S. Csonka, Phys. Rev. Lett. **115**, 227003 (2015).

<sup>15</sup> P. Samuelsson, E. V. Sukhorukov, and M. Büttiker, Phys. Rev. Lett. **91**, 157002 (2003).

<sup>16</sup> N. M. Chtchelkatchev, G. Blatter, G. B. Lesovik, and T. Martin, Phys. Rev. B **66**, 161320 (2002).

<sup>17</sup> Y. M. Blanter and M. Büttiker, Physics reports **336**, 1 (2000).

<sup>18</sup> G. Burkard, D. Loss, and E. V. Sukhorukov, Phys. Rev. B **61**, R16303 (2000).

<sup>19</sup> P. Samuelsson, E. V. Sukhorukov, and M. Büttiker, Phys. Rev. B **70**, 115330 (2004).

<sup>20</sup> B. Probst, F. Domínguez, A. Schroer, A. L. Yeyati, and P. Recher, Phys. Rev. B **94**, 155445 (2016).



- <sup>21</sup> A. C. Neto, F. Guinea, N. M. Peres, K. S. Novoselov, and A. K. Geim, *Rev. Mod. Phys.* **81**, 109 (2009).
- <sup>22</sup> C. Beenakker, *Phys. Rev. Lett.* **97**, 067007 (2006).
- <sup>23</sup> C. W. J. Beenakker, *Rev. Mod. Phys.* **80**, 1337 (2008).
- <sup>24</sup> B. L. C. Zhang and Z. Ma, *Phys. Rev. Lett.* **108**, 077002 (2012).
- <sup>25</sup> J. Cayssol, *Phys. Rev. Lett.* **100**, 147001 (2008).
- <sup>26</sup> I. Borzenets, Y. Shimazaki, G. Jones, M. F. Craciun, S. Russo, M. Yamamoto, and S. Tarucha, *Scientific reports* **6**, 23051 (2016).
- <sup>27</sup> Z. B. Tan, D. Cox, T. Nieminen, P. Lähteenmäki, D. Golubev, G. B. Lesovik, and P. J. Hakonen, *Phys. Rev. Lett.* **114**, 096602 (2015).
- <sup>28</sup> B. Uchoa and A. H. Castro Neto, *Phys. Rev. Lett.* **98**, 146801 (2007).
- <sup>29</sup> A. M. Black-Schaffer and S. Doniach, *Phys. Rev. B* **75**, 134512 (2007).
- <sup>30</sup> P. Recher and D. Loss, *Phys. Rev. B* **65**, 165327 (2002).
- <sup>31</sup> A. M. Black-Schaffer and C. Honerkamp, *J. Phys.: Condens. Matter* **26**, 423201 (2014).